Numerical Methods in Civil Engineering, 8-4 (2024) 40-46

Numerical Methods in Civil Engineering

Journal Homepage: https://nmce.kntu.ac.ir/

Application of the Image Processing Method and the Beer-Lambert Law for Assessing Sea Water Intrusion in Rivers

Ehsan Kahrizi*

ARTICLE INFO

RESEARCH PAPER

Article history:
Received:
May 2024
Revised:
June 2024
Accepted:
June 2024

Keywords:
Image Processing Method,
Sea Water Intrusion,
Beer-Lambert Law,
Density Current,
Saline Water

Abstract:

This paper presents an innovative approach integrating the Image Processing Method and the Beer-Lambert Law to study Sea Water Intrusion in riverine systems. Using an experimental setup, this study characterizes the dynamics between saline and fresh waters, providing detailed spatial and temporal salinity distribution analyses. The Beer-Lambert Law using Python is employed to convert image pixel data to accurate concentration measurements, essential for understanding the diffusion and mixing processes of saline wedges. Results showed that the concentration of the salt water is decreased when it flows upstream horizontally. also, the concentration of the saline water is decreased vertically, due to the salt and fresh water mixing. The "Max Concentration Profile" graph shows a sharp peak at the start, reaching approximately 1000 g/cm³, marking the point of saline introduction. Within the first 10 cm, the concentration rapidly decreases to about 600 g/cm³, indicating swift diffusion and dilution. Beyond this point, the concentration gradually decreases, stabilizing around 200 g/cm³ past the 100 cm mark, reflecting ongoing diffusion and mixing processes. The "Concentration Contour" graph shows high salinity concentrations near the bottom 10 cm of the flume. Salinity concentration decreases moving vertically up the flume, indicated by cooler colors. From approximately 30 cm in height, salinity remains low and uniform, suggesting that denser saline water settles at the bottom due to gravity.

1. Introduction

The phenomenon of Sea Water Intrusion (SWI) into freshwater systems is a complex hydrodynamic process with profound implications for riverine salinity distribution and ecological balance. As SWI poses a threat to biodiversity and water quality, a comprehensive understanding of salinity variations within these systems is paramount for effective water resource management [1-6]. In coastal areas, a significant portion of the water consumption is supplied by groundwater a riverain resources [7-8]. Burgan et al., (2017) conducted a statistical study about extreme events in some rivers that indicated the frequency of extreme events increased from 1981 to 2000 which can cause destructive results [9]. Overexploitation of groundwater resources, Sea-Level Rise (SLR) due to climate changes, and extreme conditions such as drought and floods lead to SWI in coastal zones [10-12]. Currently, more than 100 counties and locals worldwide are endangered by SWI [13-19].

* *Department of Civil and Environmental Engineering, Utah State University, Logan, UT, USA. Email: Ehsan.kahrizi@usu.edu*

SWI could affect water bodies and the neighboring regions along rivers; effects may include the intrusion of seawater into drinking water resources, the contamination of agricultural farms, and the pollution of groundwater resources [20-24].

Traditional methods of monitoring SWI and saline wedge through direct sampling and analysis are often constrained by their spatial and temporal limitations [25, 26]. However, the advent of image-processing technologies heralds a new paradigm for observing and quantifying these complex dynamics. The Image Processing Method (IPM) offers a non-intrusive means to assess salinity concentrations, thereby facilitating more nuanced environmental assessments [27-29]. One of the good ways to employ IPM to detect the concentration of the salinity of river water in the saline wedge is using the Beer-Lambert Law (BLL) [30-32]. This methodological integration is informed by the work of [33-39], who previously applied BLL to determine concentration profiles in flows through porous media.

Despite these technological advances, the literature reveals a notable gap in the detailed analysis of horizontal and

https://doi.org/10.61186/NMCE.2405.1058

vertical salinity variations along a seawater intrusion wedge within river systems. This knowledge is economically significant, as the extent of intrusion under real-world conditions can span tens of kilometers. Understanding the distribution of salinity along a river is essential for determining the contamination concentration at each point, which has direct implications for managing and mitigating the economic impacts of salinity intrusion. Addressing this gap, our study aims to use IPM, augmented by the quantitative power of the BLL, to characterize salinity profiles within a river flume. Thus, by blending IPM with BLL, this study not only sheds light on the patterns of SWI but also paves the way for advancements in real-time monitoring of aquatic environments. The integration of such cutting-edge technologies is vital for devising strategies to counter the challenges of freshwater depletion and underscores the importance of innovation in sustaining water resources.

2. Material and Methods

2.1 Experimental Set-up

In this experiment, a straight, 2D flume measuring 200 cm in length, 5 cm in width, and 50 cm in height was utilized (see Figure 1).

Freshwater flowed from the upstream end (right side) to the downstream end (left side). A sharp-crested weir at the reservoir's end regulated the water depth. To simulate saline wedge intrusion, seawater was introduced from an outlet at the downstream edge, flowing towards the upstream side. The experimental assumptions include a flume with zero slope and a rectangular cross-section, and no friction between the flume and the water (see Figure 2). Figure 2 shows the process of SWI over the time.

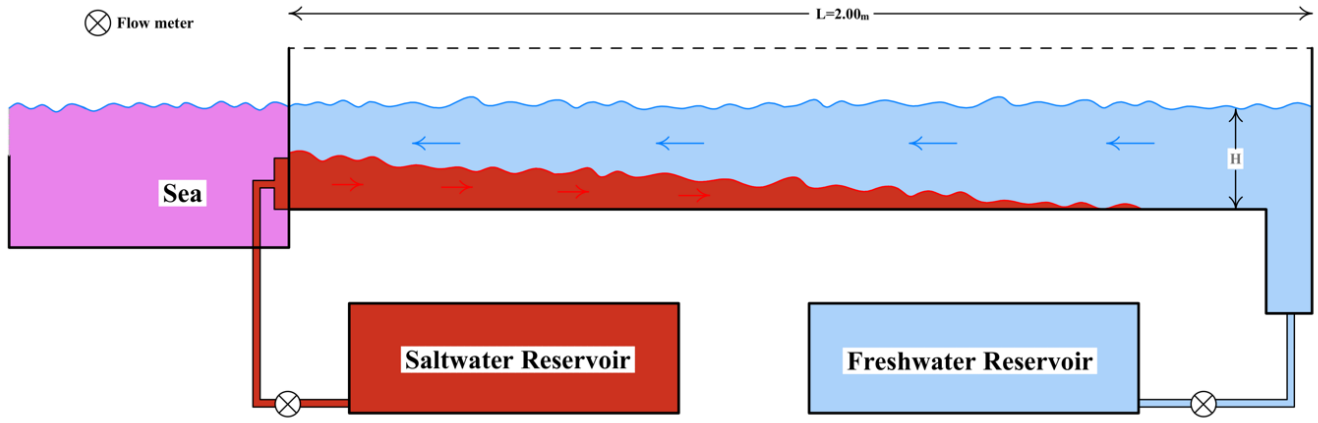

Fig. 1: Experimental set-up's side view.

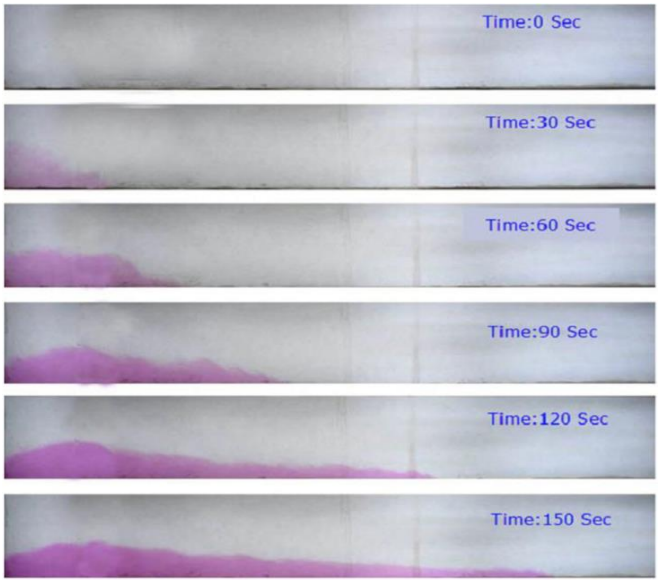

Fig. 2: SWI progress

Re_o, Fr_d, and Fr are the channel Reynolds number, channel Densimetric Froude number, and channel Froude number, respectively, which are obtained as follows (Equations 1-4):

$$Reo = \frac{q_f}{\nu} \quad (1)$$

$$Fr_d = \frac{q_f}{(g'H^3)^{0.5}} \quad (2)$$

$$g' = \left(\frac{\rho_s - \rho_f}{\rho_f}\right) * g \quad (3)$$

$$Fr = \frac{V}{(gH)^{0.5}} \quad (4)$$

where g', V, g, and ν denote the buoyancy acceleration, freshwater velocity, gravitational acceleration, and the kinematic viscosity, respectively.

2.2 Test Cases

In our experimental setup to assess the impact density of saline water on the SWI process, we designed a test case to simulate process intrusion. The test utilizes saline solutions with a density of 1.006 g/cm³. The method involves adjusting the saline water input to achieve these specific densities, thereby allowing us to study the corresponding changes in the river's salinity profile. The detail of the test case is presented in Table 1.

Table 1: Test Case details

ρ_s	Fr_d	Fr	R_{eo}
1.006	0.38	0.0307	**11277**

2.3 Image Processing Method

One important aspect of applying IPM in such studies involves quantifying the mixing levels of SWI. This quantification is achieved by correlating the pixel intensity captured in images to the dye concentration, a relationship defined by the BLL. BLL posits that the intensity of light passing through a medium is exponentially attenuated depending on the concentration of the absorbing species and the path length of the light through that medium. This law forms the theoretical foundation for determining concentration profiles in various fluids and has been particularly useful in research involving fluid flows through porous media, as demonstrated in the study by Ghisalberti & Nepf, (2005).

In practical applications within the experimental flumes, potassium permanganate serves as a tracer dye. This chemical is chosen due to its distinct color and optical properties, which make it ideal for detailed tracing of salt concentrations in seawater wedges. The presence of potassium permanganate allows for the precise determination of concentration gradients along the flume, which is crucial for understanding the mixing mechanisms at play.

For data collection, a Canon camera (Canon - EOS RP Mirrorless Camera with RF 24-105mm f/4-7.1 IS STM Lens) was used to record images of the experimental setup. These images were then processed using Python software to simulate and analyze the data. The image processing involved several preprocessing steps, including image normalization, noise reduction, and contrast enhancement, to ensure an accurate correlation between pixel intensity and dye concentration. These preprocessing steps are essential to mitigate any inconsistencies in the captured images and to enhance the precision of the subsequent analysis.

Ghisalberti & Nepf, (2005) provided a fundamental equation under BLL, where I_0 represents the initial light intensity before entering the medium, and I denote the intensity of the light after it has passed through the medium (see Figure 3). The equation is expressed as follows (Equation 5):

$$Log\left(\frac{I_0}{I}\right) = \varepsilon bc \quad (5)$$

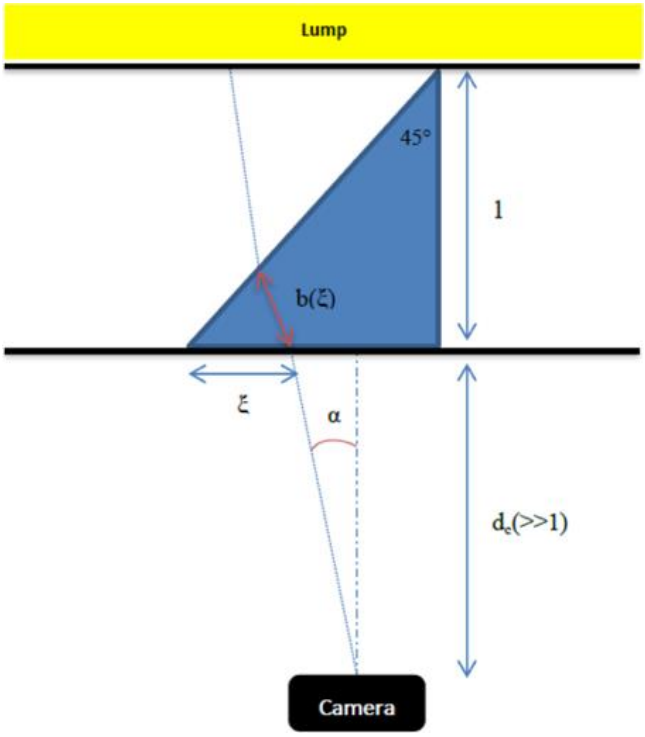

Fig. 3: Plan view of the calibration of Beer-Lambert Law in the experiments [22].

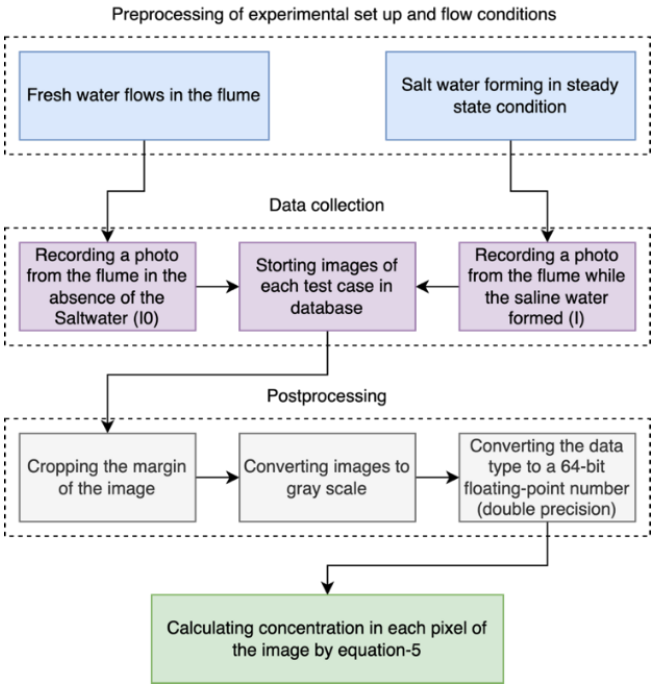

Fig. 4: Workflow of concentration of saltwater calculation.

The workflow for calculating the concentration of saltwater consists of several key stages presented in Figure 4 Initially, freshwater flows in the flume, followed by recording an image in the absence of salt water (I0). In the second part of the data collection, saltwater flows, and saltwater is formed in a steady state and the second image is recorded (I). These images are sorted and stored in a database for further analysis. The post-processing stage involves cropping the margins of the images, converting them to grayscale, and changing the data type to 64-bit floating-point numbers (double precision). The final step in the workflow is the calculation of concentration in each pixel of the images using a predefined equation, which enables precise analysis of the experimental results.

3. Results

In this study, we employed the integration of the and the BLL to investigate the phenomenon of SWI in riverine systems. The experimental setup was designed to simulate the intrusion of saline water into a river flume, capturing the complex interactions between the saline and fresh waters under controlled conditions. The resultant salinity distributions were meticulously analyzed using advanced imaging techniques and quantitative optical methods, which are instrumental in delineating the spatial and temporal variations of salinity within the flume.

Concentration Contour Analysis: Complementing the concentration profile, the "Concentration Contour" graph (Figure 5) offers a two-dimensional visualization of salinity distribution across both the length and height of the experimental setup. This graph displays a high concentration of salinity, primarily concentrated at the lower heights of the flume, especially near the bottom 10 cm, and spanning approximately the first 200 pixels in position. This high-density region correlates well with the initial peak observed in the "Max Concentration Profile" graph, reflecting the localized intensity of the saline introduction.

Concentration Profile Analysis: The "Max Concentration Profile" graph (Figure 6) vividly illustrates the dynamics of saline intrusion, beginning with a sharp peak at the start of the length scale, near the 0 cm mark, where the concentration reaches approximately 1000 g/cm³. This initial high concentration represents the point of saline introduction into the flume and is crucial for understanding the dynamics of saline mixing at the onset of intrusion. The concentration rapidly decreases to about 600 g/cm³ within the first 10 cm, demonstrating a swift diffusion and dilution process facilitated by the river's hydrodynamics. Beyond this point, the concentration continues to taper off more gradually, stabilizing around 200 g/cm³ past the 100 cm mark. This profile not only provides insights into the initial impact of the saline intrusion but also into the subsequent dispersion and mixing processes as the saline water travels downstream. The decreasing trend observed along the length of the flume is indicative of the diffusion and mixing processes affecting the saltwater as it integrates with the river water, progressively diluting as it moves away from the source.

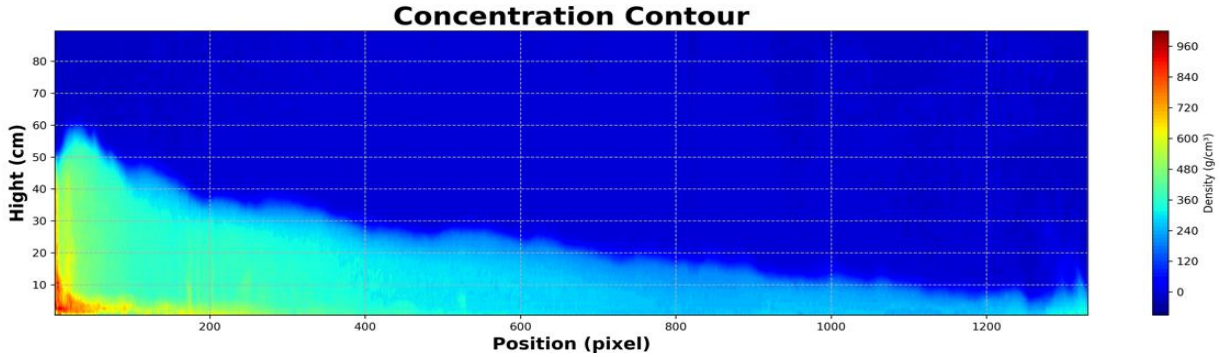

Fig. 5: Concentration Contour

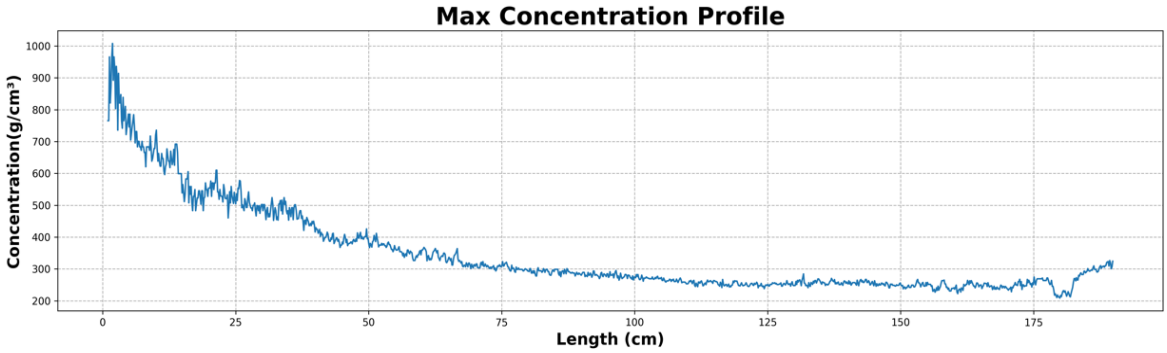

Fig. 6: Max Concentration Profile

As one moves vertically up the flume from this initial high concentration zone, there is a noticeable transition to lower concentrations, depicted in cooler colors such as blue, indicating lesser salinity. Notably, from approximately 30 cm in height, the salinity concentration remains relatively low and uniform across the remainder of the flume. This vertical stratification of salt concentration is indicative of the denser saline water settling at the bottom of the flume due to gravitational forces, with less mixing occurring at higher elevations. The clearer waters above demonstrate less interference from the saline water, highlighting the effectiveness of natural stratification processes in containing and isolating saline intrusions at lower levels.

4. Discussion

In this study, the integration of the IPM and the BLL provided pivotal insights into the dynamics of SWI within riverine systems, particularly emphasizing the interaction between saline and fresh waters. The "Max Concentration Profile" and "Concentration Contour" graphs were instrumental in validating the BLL's theoretical predictions about light attenuation through varying concentrations of saline solutions. Observations from the experimental setup revealed an initial high concentration of salinity at the point of introduction, which exhibited an exponential decrease in concentration as it progressed downstream, aligning with BLL expectations where light absorption is most intense near the source of saline intrusion.

The spatial distribution captured in these visualizations crucially demonstrated the effectiveness of combining IPM and BLL for real-time environmental monitoring, offering a non-intrusive means to continuously analyze the extent of saltwater intrusion. Such monitoring is vital for managing water resources in coastal areas, where the dynamics of saline intrusion are a major concern. Additionally, the stratification pattern observed in the "Concentration Contour" graph aligns with BLL predictions, showing that the denser saline layer remained settled at the bottom due to gravitational forces, thereby reducing light penetration and increasing absorption in these lower layers.

This stratification is critical for understanding saline intrusion dynamics, especially in scenarios where the saline water's density surpasses that of freshwater. The results from this study provide valuable insights into the mechanisms controlling saltwater propagation and mixing, which are essential for developing strategies to mitigate the impact of saline intrusion on river water quality-a factor crucial for both ecological health and human consumption.

Moreover, by employing IPM and BLL, the study highlights the potential of merging advanced technological methods with classical physical laws to enhance our comprehension of complex environmental phenomena. This approach not only confirms BLL's utility in environmental studies but also underscores the importance of sophisticated imaging and analytical techniques in hydrological research.

The comprehensive analysis provided by this integration not only advances our theoretical knowledge of SWI dynamics but also equips water resource managers with empirical data and practical insights. These insights are indispensable for forecasting changes and implementing effective countermeasures against the adverse effects of saline water intrusion into freshwater systems. Ultimately, this study underscores the significance of such innovative methodologies in promoting sustainable water resource management in regions susceptible to saline intrusion.

5. Conclusion

This study combined the IPM and the BLL to investigate SWI in river systems. Using a new experimental setup, it offered detailed insights into the interactions between saline and freshwater, demonstrating how saline water disperses within a river flume. The application of IPM and BLL allowed for real-time monitoring of salinity distributions, critical for managing water resources effectively in coastal areas. This approach confirmed theoretical models about light attenuation related to saline concentrations and provided a deeper understanding of the diffusion processes and behaviors of saline wedges.

The research showed that combining IPM with BLL could revolutionize environmental monitoring by providing non-intrusive, precise, and ongoing evaluations of water salinity. This synergy is crucial for the strategic management of water resources, helping to mitigate the impact of SWI. The study highlights the role of technological advancements in hydrology, combining modern imaging techniques with traditional analytics to enhance theoretical and practical understanding of environmental challenges. Ultimately, the study underlines the potential of integrating advanced technology with scientific principles to improve the management and sustainability of water resources in regions prone to saline intrusion.

However, this study also has its limitations. The experimental conditions were based on certain assumptions, such as the absence of sediment and vegetation in the water, which may not fully represent natural river systems. Future research could explore the effects of these factors on SWI to provide a more comprehensive understanding. Additionally, the study utilized saltwater with a single specific concentration. Investigating different levels of salinity could yield valuable insights into the effects of varying salinity densities on dispersion processes.

By addressing these limitations, future studies can further refine the experimental setup and image processing methodology, enhancing the accuracy and applicability of

the findings. These improvements would contribute to a deeper and more nuanced understanding of SWI, ultimately aiding in the development of more effective strategies for managing water resources in coastal and estuarine environments.

References

[1] Kahrizi, O., Naderi, N., Rezaei, B., & Olya, H. (2020). The Barriers Against the Entrepreneurship Development of Medical and Healthcare Tourism Industry: Evidence from Kermanshah, Iran. International Journal of Health and Life Sciences, 6(2). https://doi.org/10.5812/ijhls.102036

[2] Rezapouraghdam, H., Kahrizi, O., & Hassannia, R. (2015). On The Right Path towards Benefiting From Tourism; A Compendious Debate on Sustainability. Journal of Sustainable Development Studies, 8(1), 37–52. www.northcyprus.cc

[3] Heidarian, P., Neyshabouri, S. A. A. S., Khoshkonesh, A., Bahmanpouri, F., Nsom, B., & Eidi, A. (2022). Numerical study of flow characteristics and energy dissipation over the slotted roller bucket system. Modeling Earth Systems and Environment, 8(4), 5337–5351. https://doi.org/10.1007/s40808-022-01372-z

[4] Bonomelli, R., Pilotti, M., & Heidarian, P. (2024). DEBRA: A multi-rheological 2D steep shallow water finite volume scheme for debris flow propagation in mountain areas. EGU General Assembly 2024, Vienna, Austria, 14–19 April 2024. https://doi.org/10.5194/egusphere-egu24-4141

[5] Kahrizi, O., Naderi, N., Rezaei, B., & Olya, H. (2021). Identifying and Prioritizing Components of the Medical and Healthcare Tourism Entrepreneurship Ecosystem. Health Management & Information Science, 8(1), 16–26.

[6] Souri, J., Akbari, H., Salehi Neyshabouri, S. A. A., & OmidvarMohammadi, H. (2023). A Study of Nappe Oscillations and Effects of Aeration on Environmental Noise of Piano Key Weirs with Different Shapes. Iranian Journal of Science and Technology, Transactions of Civil Engineering, 47(3), 1813–1830.

[7] Erostate, M., Huneau, F., Garel, E., Ghiotti, S., Vystavna, Y., Garrido, M., & Pasqualini, V. (2020). Groundwater dependent ecosystems in coastal Mediterranean regions: Characterization, challenges and management for their protection. Water Research, 172, 115461. https://doi.org/10.1016/j.watres.2019.115461

[8] Hajebi, Z., Firozjaei, M. R., Naeeni, S. T. O., & Akbari, H. (2024). Hydraulic performance of bottom intake velocity caps using PIV and OpenFOAM methods. Applied Water Science, 14(3), 38. https://doi.org/10.1007/s13201-023-02091-1

[9] Burgan, H. I., Vaheddoost, B., & Aksoy, H. (2017). Frequency Analysis of Monthly Runoff in Intermittent Rivers. World Environmental and Water Resources Congress 2017, 327–334. https://doi.org/10.1061/9780784480625.030

[10] Ebrahimi, E., & Shourian, M. (2020). River Flow Prediction Using Dynamic Method for Selecting and Prioritizing K-Nearest Neighbors Based on Data Features. Journal of Hydrologic Engineering, 25(5). https://doi.org/10.1061/(asce)he.1943-5584.0001905

[11] Firozjaei, M. R., Hajebi, Z., Naeeni, S. T. O., & Akbari, H. (2024). Discharge performance of a submerged seawater intake in unsteady flows: Combination of physical models and decision tree algorithms. Journal of Water Process Engineering, 60, 105198. https://doi.org/10.1016/j.jwpe.2024.105198

[12] Benetti, M., Heidarian, P., Bonomelli, R., & Pilotti, M. (2024). Exploring remote sensing methodologies for river bed grain size: Insights from a mountainous watershed study in Val Camonica, Italy. EGU General Assembly 2024, Vienna, Austria, 14–19 April 2024. https://doi.org/10.5194/egusphere-egu24-5752

[13] Abd-Elhamid, H., Javadi, A., Abdelaty, I., & Sherif, M. (2016). Simulation of seawater intrusion in the Nile Delta aquifer under the conditions of climate change. Hydrology Research, 47(6), 1198–1210.

[14] Barlow, P. M., & Reichard, E. G. (2010). Saltwater intrusion in coastal regions of North America. Hydrogeology Journal, 18(1), 247–260. https://doi.org/10.1007/s10040-009-0514-3

[15] Bhagat, C., Khandekar, A., Singh, A., Mohapatra, P. K., & Kumar, M. (2021). Delineation of submarine groundwater discharge and seawater intrusion zones using anomalies in the field water quality parameters, groundwater level fluctuation and sea surface temperature along the Gujarat coast of India. Journal of Environmental Management, 296, 113176. https://doi.org/10.1016/j.jenvman.2021.113176

[16] Han, D., & Currell, M. J. (2018). Delineating multiple salinization processes in a coastal plain aquifer, northern China: hydrochemical and isotopic evidence. Hydrology and Earth System Sciences, 22(6), 3473–3491.

[17] Motaei, S., Ghazavi, M., & Rezazadeh, G. (2024). Incorporating temperature-dependent properties into the modeling of photo-thermo-mechanical interactions in cancer tissues. Thermal Science and Engineering Progress, 47, 102351. https://doi.org/10.1016/j.tsep.2023.102351

[18] Palacios, A., Ledo, J. J., Linde, N., Luquot, L., Bellmunt, F., Folch, A., Marcuello, A., Queralt, P., Pezard, P. A., Mart\'\inez, L., & others. (2020). Time-lapse cross-hole electrical resistivity tomography (CHERT) for monitoring seawater intrusion dynamics in a Mediterranean aquifer. Hydrology and Earth System Sciences, 24(4), 2121–2139.

[19] Firozjaiy, M. R., Talab, E. B., & Neyshabouri, S. A. A. S. (2019). Numerical simulation of lateral pipe intake from open channel. Iran J Soil Water Res, 50(1), 135–147.

[20] Roudbari, M. V., Dehnavi, A., Jamshidi, S., & Yazdani, M. (2023). A multi-pollutant pilot study to evaluate the grey water footprint of irrigated paddy rice. Agricultural Water Management, 282, 108291.

[21] Khoshkonesh, A., Nsom, B., Ahmadi Dehrashid, F., Heidarian, P., & Riaz, K. (2021). Comparison of the SWE and 3D models in simulation of the dam-break flow over the mobile bed. https://www.researchgate.net/publication/353283892

[22] Kahrizi, E., Salehi Neyshabouri, S. A. A., Zeynolabedin, A., Souri, J., & Akbari, H. (2023). Experimental evaluation of two-layer air bubble curtains to prevent seawater intrusion into rivers. Journal of Water and Climate Change, 14(2), 543–558. https://doi.org/10.2166/wcc.2023.384

[23] Rezapouraghdam, H., Shahgerdi, A., & Kahrizi, O. (2015). An introduction to edu-tourism in Northern Cyprus: A short communication. International Journal of Sciences: Basic and Applied Research, 19(2), 92–98.

[24] Rahmani Firozjaei, M., Behnamtalab, E., & Salehi Neyshabouri, S. A. A. (2020). Numerical simulation of the lateral pipe intake: flow and sediment field. Water and Environment Journal, 34(2), 291–304.

[25] Ebrahimi, E., & Shourian, M. (2022). A feature-based adaptive combiner for coupling meta-modelling techniques to increase accuracy of river flow prediction. Hydrological Sciences Journal, 67(14), 2065–2081. https://doi.org/10.1080/02626667.2022.2130700

[26] Khoshkonesh, A., Nsom, B., Okhravi, S., Ahmadi Dehrashid, F., Heidarian, P., & DiFrancesco, S. (2024). Numerical investigation of dam break flow over erodible beds with diverse substrate level variations. Journal of Hydrology and Hydromechanics, 72(1), March 2024. https://doi.org/10.2478/johh-2023-0040

[27] Khoshkonesh, A., Asim, T., Mishra, R., Dehrashid, F. A., Heidarian, P., & Nsom, B. (2022). Study the effect of obstacle arrangements on the dam-break flow. International Journal of COMADEM. https://pure.hud.ac.uk/ws/files/47608562/Alireza_etal_COMADEM_final_5_1_.pdf

[28] Rahmani firozjaei, M., hajebi, Z., Naeeni, S. T. O., & Akbari, H. (2024). Experimental and Numerical Investigation of Bottom Intake Structure for Desalination Plants. Numerical Methods in Civil Engineering, *8*(3), 1-9. doi: 10.52547/NMCE.2303.1022

[29] Rahmani Firozjaei, M., & Behnamtalab, E. (2021). Hydraulic Evaluation of Lateral Pipe-intake from Open Channel by Numerical Simulation. Modares Civil Engineering Journal, 21(3), 45–60.

[30] Swinehart, D. F. (1962). The beer-lambert law. Journal of chemical education, 39(7), 333.

[31] Khoshkonesh, A., Nsom, B., Dehrashid, F. A., Heidarian, P., & Riaz, K. (2021, January). Comparison of the SWE and 3D models in simulation of the dam-break flow over the mobile bed. In Fifth scientific Conference of applied research in science and technology of Iran.

[32] Naeeni, S. T. O., Rahmani Firozjaei, M., Hajebi, Z., & Akbari, H. (2023). Investigation of the performance of the response surface method to optimize the simulations of hydraulic phenomena. Innovative Infrastructure Solutions, 8(1), 10.

[33] Ghisalberti, M., & Nepf, H. (2005). Mass transport in vegetated shear flows. Environmental Fluid Mechanics, 5(6), 527–551. https://doi.org/10.1007/s10652-005-0419-1

[34] Ghaffari, S. B., & Tavakoli, O. (2022). Industrial waste generation and characterization in Iran: a circular economy approach. http://generalchemistry.chemeng.ntua.gr/uest/corfu2022/proceedings/II/1345_Valiasil.pdf

[35] Firozjaei, M. R., Naeeni, S. T. O., & Akbari, H. (2023). Evaluation of seawater intake discharge coefficient using laboratory experiments and machine learning techniques. Ships and Offshore Structures, 1–14. https://doi.org/10.1080/17445302.2023.2247125

[36] Rahmani Firozjaei, M., Salehi Neyshabouri, S.A.A., Amini Sola, S. and Mohajeri, S.H., 2019. Numerical simulation on the performance improvement of a lateral intake using submerged vanes. *Iranian Journal of Science and Technology, Transactions of Civil Engineering*, *43*, pp.167-177.

[37] Yavari, F., Salehi Neyshabouri, S. A., Yazdi, J., Molajou, A., & Brysiewicz, A. (2022). A novel framework for urban flood damage assessment. Water Resources Management, 36(6), 1991–2011.

[38] Kahrizi, E. (2024). Application of the Image Processing Method and the Beer-Lambert Law for Assessing Sea Water Intrusion in Rivers. EarthArXiv. https://doi.org/10.31223/X50D8K

[39] Souri, J., OmidvarMohammadi, H., Neyshabouri, S.A.A.S., Chooplou, A.C, Kahrizi, E, & Akbari, H. (2024). Numerical simulation of aeration impact on the performance of a-type rectangular and trapezoidal piano key weirs. Modeling Earth Systems and Environment. https://doi.org/10.1007/s40808-024-02058-4